Toxicology Reports 8 (2021) 1721–1728

Contents lists available at ScienceDirect

Toxicology Reports

journal homepage: www.elsevier.com/locate/toxrep

Effect of tannic acid-templated mesoporous silica nanoparticles on iron-induced oxidative stress and liver toxicity in rats

Hossein Javdani [a,g], Leila Etemad [b], Mohammad Moshiri [c], Asghar Zarban [d,e,**], Mohammad Yahya Hanafi-Bojd [a,f,*]

[a] Cellular and Molecular Research Center, Birjand University of Medical Sciences, Birjand, Iran
[b] Pharmaceutical Research Center, Pharmaceutical Technology Institute, Mashhad University of Medical Sciences, Mashhad, Iran
[c] Medical Toxicology Research Center, Mashhad University of Medical Sciences, Mashhad, Iran
[d] Cardiovascular Diseases Research Center, Birjand University of Medical Sciences, Birjand, Iran
[e] Clinical Biochemistry Department, Faculty of Medicine, Birjand University of Medical Sciences, Birjand, Iran
[f] Nanomedicine Department, Faculty of Medicine, Birjand University of Medical Sciences, Birjand, Iran
[g] Molecular Medicine Research Center, Research Institute of Basic Medical Sciences, Rafsanjan University of Medical Sciences, Rafsanjan, Iran

ARTICLE INFO

Handling Editor: Dr. Aristidis Tsatsakis

Keywords:
Acute iron toxicity
Antioxidant activity
Liver damage
Mesoporous silica nanoparticles
Oxidative stress
Tannic acid

ABSTRACT

The present study sought to investigate the effects of amino-functionalized tannic acid-templated mesoporous silica nanoparticles (TA-MS-NH_2 NPs) on giving rats protection against iron-induced liver toxicity. To this end, the TA-MS-NH_2 NPs were characterized using field-emission scanning electron microscope (FE-SEM), transmission electron microscopy (TEM), dynamic light scattering (DLS), and Fourier-transform infrared spectroscopy (FTIR). Moreover, 50 Wistar rats were randomly divided into one control group (group 1) and four experimental groups (groups 2- 5) (n = 10), each of which received 100 mg/kg oral normal saline and $FeSO_4$, respectively. Then, post-exposure hepatotoxicity and oxidative stress markers were measured in two intervals, i.e., after 4 and 24 h, followed by the measurement of the acute iron toxicity. Furthermore, hepatotoxicity markers, including the alanine aminotransferase (ALT), aspartate aminotransferase (AST), alkaline phosphatase (ALP), and total antioxidant capacity (TAC), were measured via Ferric Reducing Antioxidant Power (FRAP) and 2,2,1-diphenyl-1-picrylhydrazyl (DPPH) assays. Also, malondialdehyde (MDA), total thiol groups, advanced oxidation protein products (AOPP), and nitrite/nitrate (NOx) levels were measured as oxidative stress markers in the serum samples. The results indicated that oral administration of iron significantly elevated the liver enzymes and altered the level of oxidative stress markers. It was also found that treatment with TA-MS-NH_2 NPs meaningfully protected against hepatotoxicity, decreased ALT, AST, ALP, and significantly improved oxidative stress markers by decreasing MDA, AOPP, and NOx levels and increasing TAC and thiol group contents, proving that TA-MS-NH_2 NPs could protect rats against iron-induced acute liver toxicity through their antioxidant features.

1. Introduction

Iron is known as a bio-element transition metal. However, inadequate or excessive intake of this essential micronutrient may cause physical pathological changes [1]. Therefore, while low levels of iron (less than 20 mg/daily) are necessary for the human body, 20–60 mg/kg intake of iron can bring about moderate intoxication symptoms, and more than 60 mg/kg may lead to severe morbidity and mortality [2]. As found by different studies, shock and liver failure are among the most common problems caused by iron intoxication [3].

In the United States, approximately 11,000 cases of iron exposures are documented among children under 5 years annually [4]. However,

Abbreviations: TA-MS-NH_2 NPs, amino-functionalized tannic acid-templated mesoporous silica nanoparticles; FE-SEM, field-emission scanning electron microscope; TEM, transmission electron microscopy; DLS, dynamic light scattering; FT-IR, Fourier-transform infrared spectroscopy; ALT, alanine aminotransferase; AST, aspartate aminotransferase; ALP, alkaline phosphatase; TAC, total antioxidant capacity; MDA, malondialdeide; AOPP, advanced oxidation protein products; FRAP, Ferric Reducing Antioxidant Power; DPPH, 2,2,1-diphenyl-1-picrylhydrazyl.

* Corresponding author at: Nanomedicine department, Faculty of Medicine, Birjand University of Medical Sciences, Birjand, Iran.
** Corresponding author at: Department of Biochemistry, Faculty of Medicine, Birjand University of Medical Sciences, Birjand, 9717853577, Iran.
E-mail addresses: azarban@bums.ac.ir (A. Zarban), myhanafibojd@bums.ac.ir (M.Y. Hanafi-Bojd).

https://doi.org/10.1016/j.toxrep.2021.09.005
Received 11 May 2021; Received in revised form 11 September 2021; Accepted 30 September 2021
Available online 1 October 2021

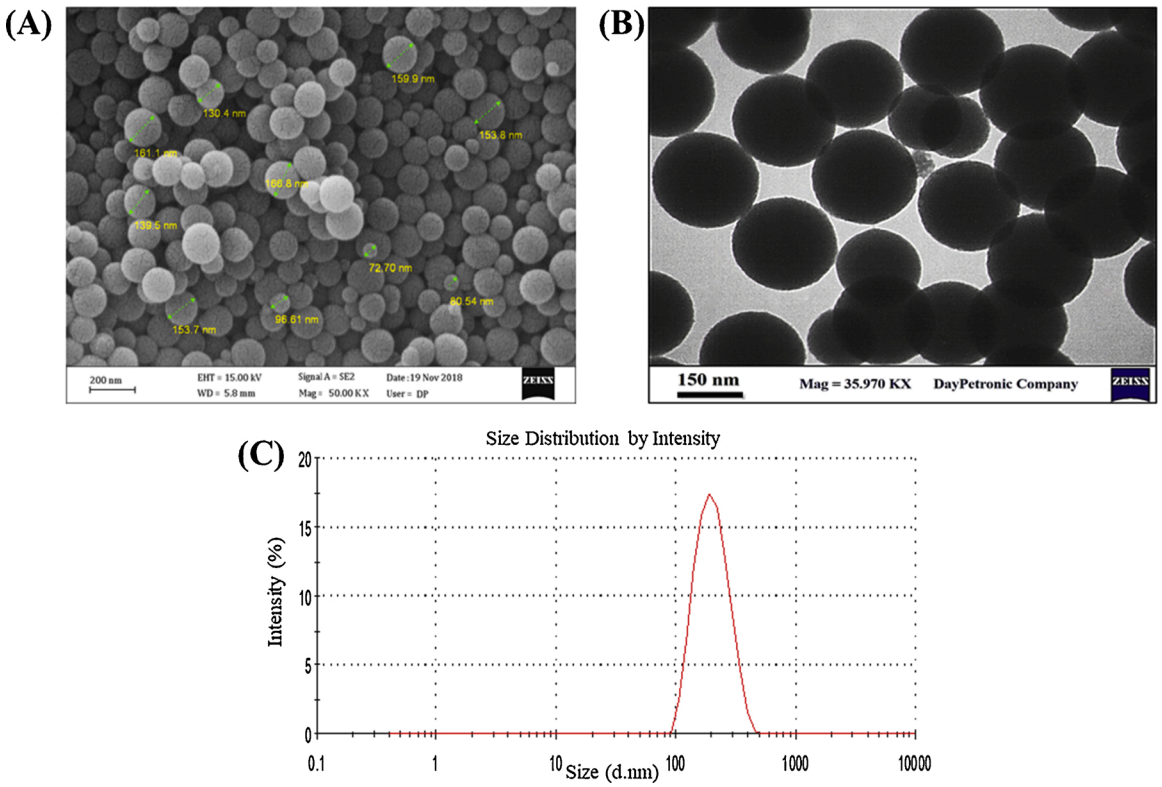

Fig. 1. FE-SEM images of TA-MS-NH_2 NPs (A), TEM images of TA-MS-NH_2 NPs (B), and Size profiles of TA-MS-NH_2 NPs (C).
Abbreviations: TA-MS-NH_2 NPs: Amino-functionalized tannic acid-templated mesoporous silica nanoparticles; FE-SEM: Field emission scanning electron microscopy; TEM: Transmission electron microscopy.

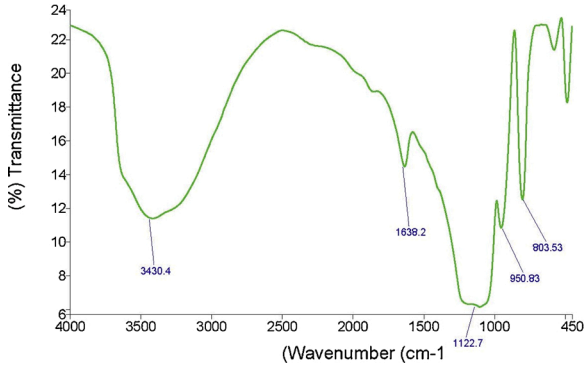

Fig. 2. FT-IR spectra of the amino-functionalized tannic acid-templated mesoporous silica nanoparticles (TA-MS-NH_2 NPs).

although the number of child deaths has currently been decreased, there is still high mortality caused by intentional or accidental iron ingestions, indicating significant toxicity of iron supplements [5].

Oxidative stress and the imbalance among the antioxidant defense are well known as the mechanism of iron overload toxicity, that accelerates the reactive oxygen species (ROS) production [6,7], that in turn may damage various cellular biomolecules such as carbohydrates, proteins, lipids, and polynucleotides, causing disease initiation and progression [9,10]. In this regard, the toxic effect of iron overload seems to be mainly associated with its participation in the Haber-Weiss and Fenton reactions that generate ROS species [8].

In contrast to iron absorption and recycling, there is no excretory mechanism for excess iron in mammalian bodies [11]. The most common treatments for excess iron include phlebotomy and erythrocytapheresis that are associated with rapid elimination of iron overload as hemoglobin and chelating drugs that bind selectively to iron and increase the removal of excess iron from the body [12]. Unfortunately, such treatments have multiple limitations and undesirable effects [12,13]. However, mesoporous silica nanoparticles (MS NPs) have recently received increasing attention in the nanomedicine field due to their unique intrinsic features [14,15]. As one of the most important classes of nanomaterials with ROS scavenging, MS NP has proved to have a protective effect on oxidative stress [16].

Many studies have so far been conducted on the preparation of MS NPs through neutral surfactants or non-surfactant templates such as tannic acid [17], tartaric acid [18], and boron oxide [19], out of which tannic acid has attracted more attention in recent years. Unlike expensive and toxic surfactants applied in traditional methods to prepare MS NPs, tannic acid is an inexpensive, non-surfactant molecule, eco-friendly, and effective antioxidant component used in preparing MS NPs [20].

As an effective natural antioxidant component, tannic acid has widely been researched in recent years [21]. While the antioxidant activity of tannic acid was previously proved to be associated with its ability to form a complex with Fe (II) and prevent the Fenton reaction [22], recent studies have shown the protective effect of tannic acid against free-radical formation and ROS scavenging [22–24]. Moreover, although some studies have suggested the protective effect of TA-MS-NH_2 NPs [25], its positive effect on iron-induced hepatotoxicity has not been established. Therefore, the present study sought to synthesize TA-MS-NH_2 NPs, determine their unique properties, and examine the antioxidant capacity of TA-MS-NH_2 NPs against iron-induced hepatotoxicity in rats.

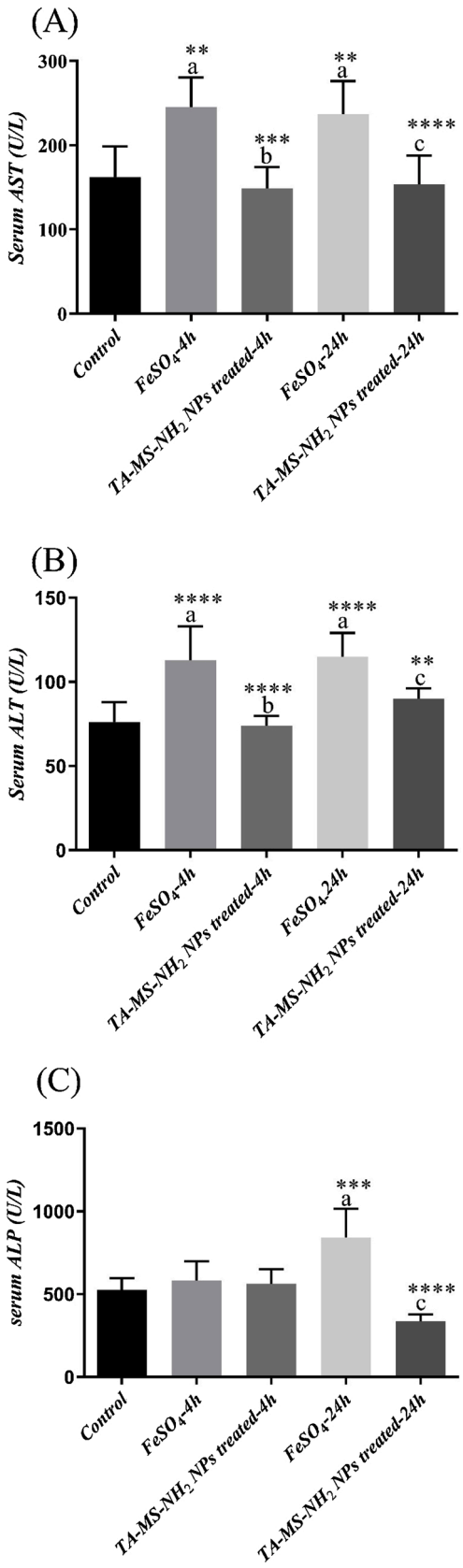

(caption on next column)

Fig. 3. Effect of $FeSO_4$ and TA-MS-NH_2 NPs on serum AST (A), ALT (B), and ALP (C) enzymes in rats. Rats treated with iron indicated an increased in the levels of serum marker enzymes. Treatment with TA-MS-NH_2 NPs significantly decreased mentioned serum marker levels. The results are reported as the mean ± standard deviation (SD). a) Significant difference vs. control group, b) Significant difference vs. the $FeSO_4$-4 h group, c) Significant difference vs. the $FeSO_4$-24 h group; **, $p < 0.01$, ***, $p < 0.001$ and ****, $p < 0.0001$.
Abbreviations: TA-MS-NH_2 NPs: Amino-functionalized tannic acid-templated mesoporous silica nanoparticles; $FeSO_4$: Ferrous sulfate; ALT: Alanine aminotransferase; AST: Aspartate aminotransferase; ALP: Alkaline phosphatase.

2. Material and methods

2.1. Materials

Tetraethyl orthosilicate (TEOS), 3-Aminopropyltriethoxysilane (APTES), sodium acetate trihydrate, acetic acid ($C_2H_4O_2$), 2,4,6-tripyridyl- s-triazine (TPTZ), and tannic acid powder were purchased from Sigma-Aldrich (USA). Iron (II) sulfate heptahydrate ($FeSO_4.7H_2O$), ammonia solution (32 %), methanol (99.9 %), and ethanol (96 %) were purchased from MERCK. Then, the aspartate aminotransferase (AST), alanine aminotransferase (ALT), and Alkaline Phosphatase (ALP) were measured via the enzymatic method by Pars Azmoon (Tehran, Iran) kits. Moreover, the Ferric Reducing Antioxidant Power (FRAP), 2,2,1-diphenyl-1-picrylhydrazyl (DPPH), Thiobarbituric acid reactive substances (TBARS), thiol groups, and Advanced Oxidation Protein Products (AOPP) assay kits were obtained from Zantox (Birjand, Iran). Finally, the total nitric oxide kit was purchased from ZellBio GmbH (Germany).

2.2. Preparation of TA-MS-NH_2 NPs

The nanoparticle synthesis was conducted based on the method presented by Jiang and colleagues [26,27]. To synthesize TA-MS-NH_2 NPs, 408 mg tannic acid was dissolved in 300 mL ethanol and stirred for about 5 min, and then the 150 mL ammonia solution was added under stirring. After 30 min, APTES (360 μL) was mixed with 1.8 mL of TEOS and ethanol, which was then, added dropwise to the tannic acid solution in an inert atmosphere. After vigorous stirring for 2 h, the gray precipitate was separated by centrifugation and washed with methanol solution. Then, these products were washed 5 times with water/methanol solutions to remove the free tannic acid. Finally, the precipitates were dried in a vacuum desiccator at ambient temperature.

2.3. Characterization methods

2.3.1. Particle size and zeta potential measurement

Hydrodynamic size, polydispersity index (PDI), and zeta potential of the synthesized TA-MS-NH_2 NPs were characterized through dynamic light scattering (DLS) measurements using a Zetasizer Nano ZS (Malvern Instruments, UK). Before measurements, all samples were suspended in deionized (DI) water and sonicated for 10 min. The size distribution curves were reported in the intensity mode.

2.3.2. Morphology determination

The shape, size, and structure of the synthesized TA-MS-NH2 NPs were analyzed using Field Emission Scanning Electron Microscope (FE-SEM) and transmission electron microscopy (TEM) (Zeiss, EM10C, Germany).

2.3.3. Fourier-transform infrared (FT-IR) spectroscopy measurements

TA-MS-NH_2 NPs' FT-IR spectrum was obtained using KBr-pressed disk in the 4000–450 cm^{-1} range (Perkin–Elmer, USA).

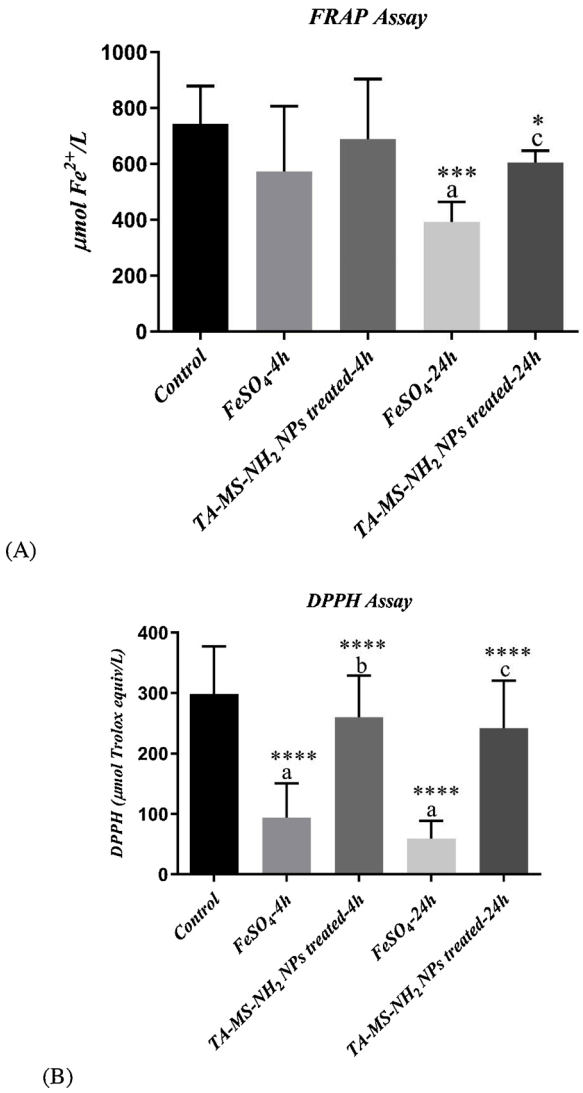

Fig. 4. Effect of TA-MS-NH_2 NPs on iron overload induced hepatotoxicity evaluated by using total antioxidant capacity after 4 and 24 h. (A) FRAP; and (B) DPPH assays. Quantitative data are reported as the mean ± standard deviation (SD). a) Significant difference vs. the control group, b) Significant difference vs. the $FeSO_4$-4 h group, c) Significant difference vs. the $FeSO_4$-24 h group ; *, $p < 0.05$; **, $p < 0.01$ and ***, $p < 0.001$.

Abbreviations: TA-MS-NH_2 NPs: Amino-functionalized tannic acid-templated mesoporous silica nanoparticles; $FeSO_4$: Ferrous sulfate; FRAP: Ferric reducing antioxidant power; DPPH: 2,2′-diphenyl-1-picrylhydrazyl.

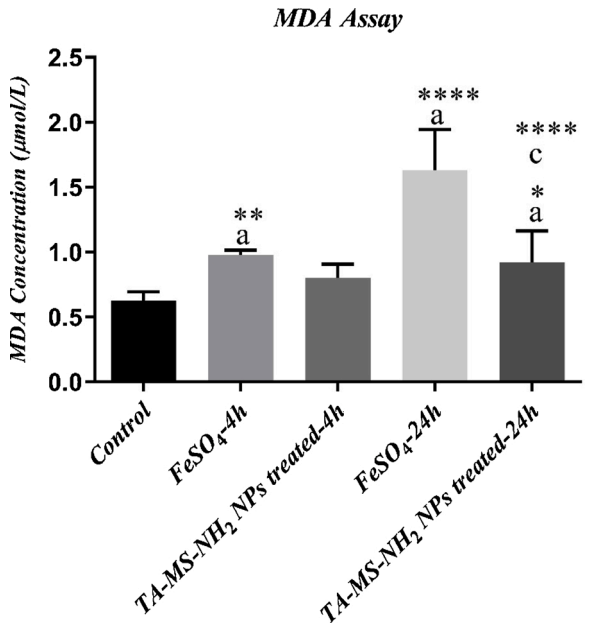

Fig. 5. Effect of TA-MS-NH_2 NPs in iron overload induced hepatotoxicity evaluated by using MDA level after 4 and 24 h. MDA levels increased in $FeSO_4$-4 h and $FeSO_4$-24 h groups compared with the control group. Treatment with TA-MS-NH_2 NPs after 24 h meaningfully decreased MDA levels in TA-MS-NH2 NPs treated-24 h group compared with $FeSO_4$-24 h group. Quantitative data are reported as the mean ± standard deviation (SD). a) Significant difference vs. control group, c) Significant difference vs. the FeSO4-24 h group; *, $p < 0.05$; **, $p < 0.01$ and ****, $p < 0.0001$.

Abbreviations: MDA; Malondialdehyde levels, $FeSO_4$: Ferrous sulfate; TA-MS-NH_2 NPs: Amino-functionalized tannic acid-templated mesoporous silica nanoparticles.

2.4. Experimental design

Fifty male Wistar rats (200–250 g body weight) were provided from the Animal Laboratory for Experimental Medicine Research Center, Birjand University of Medical Sciences. The rats were housed on a 12 h alternating light-dark cycle at a constant temperature (22 ± 1 °C) with free access to pellets and fresh water. This study was accepted by the ethical committee of Birjand University of Medical Sciences (ID: Ir.bums.REC.1398.352).

The rats were randomly divided into 5 groups (n = 10 rats per group) as follows:

Group 1: Control (normal saline)

Group 2: Acute iron toxicity induced by $FeSO_4$ (100 mg/kg body weight), was evaluated after 4 h. ($FeSO_4$-4 h)

Group 3: Acute iron toxicity induced by $FeSO_4$ (100 mg/kg body weight), was treated by TA-MS-NH_2 NPs (1 g/kg) after 30 min and evaluated after 4 h. (TA-MS-NH2 NPs treated-4 h)

Group 4: Acute iron toxicity induced by $FeSO_4$ (100 mg/kg body weight), and it was evaluated after 24 h. ($FeSO_4$-24 h)

Group 5: Acute iron toxicity induced by $FeSO_4$ (100 mg/kg body weight), treated by TA-MS-NH_2 NPs (1 g/kg) after 30 min and evaluated after 24 h. (TA-MS-NH2 NPs treated-24 h)

Eventually, the rats' serum samples were collected after 4 or 24 h to evaluate hepatotoxicity and oxidative stress markers.

2.5. Serum biochemical measurement

The levels of serum liver enzymes (AST, ALT, and ALP) were measured by a Chemistry Analyzer (Tokyo Boeki Prestige 24i) using commercially available kits (Pars Azmoon, Tehran, Iran).

2.6. Measurement of antioxidant parameters

2.6.1. Total antioxidant activity (TAC) measurement

2.6.1.1. FRAP assay. The FRAP assay, first introduced by Benzie et al. [28] as a direct procedure for assessing the TAC, assesses the antioxidant capacity of samples in reducing Fe^{3+} (ferric ion) to Fe^{2+} (ferrous ion) [29]. Thus, the TPTZ working solution was prepared in this study by mixing 25 mL reaction buffer, 2.5 mL Fe^{+3} ion reaction, and 2.5 ml TPTZ solution. Using Zantox kits (Birjand, Iran), 250 µL freshly-prepared TPTZ working solution was added to 10 µL of samples in microplate wells, and it was kept at 37 °C. After 15 min, the absorbance was recorded at a wavelength of 593 nm. The results were expressed as µmol/L.

2.6.1.2. DPPH assay. The scavenging capacity of DPPH radical was measured by using Zantox kits (Birjand, Iran) and the slightly modified

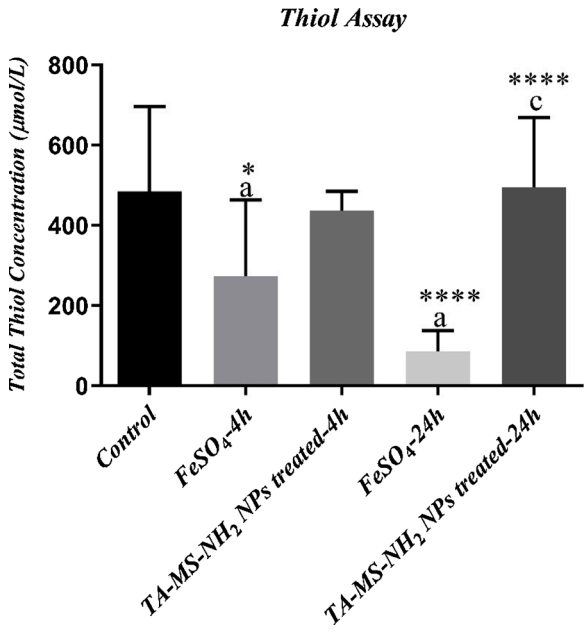

Fig. 6. Effect of TA-MS-NH_2 NPs in iron overload induced hepatotoxicity evaluated by using thiol level after 4 and 24 h. Thiol content decreased in $FeSO_4$-treated rats compared with the control group. Treatment with TA-MS-NH_2 NPs after 24 h meaningfully increased the thiol levels in TA-MS-NH2 NPs treated-24 h group compared with the $FeSO_4$-24 h group. Quantitative data are reported as the mean ± standard deviation (SD). a) Significant difference vs. control group, c) Significant difference vs. the FeSO4-24 h group; *, $p < 0.05$ and ****, $p < 0.001$.

Abbreviations: $FeSO_4$: Ferrous sulfate; TA-MS-NH_2 NPs: Amino-functionalized tannic acid-templated mesoporous silica nanoparticles.

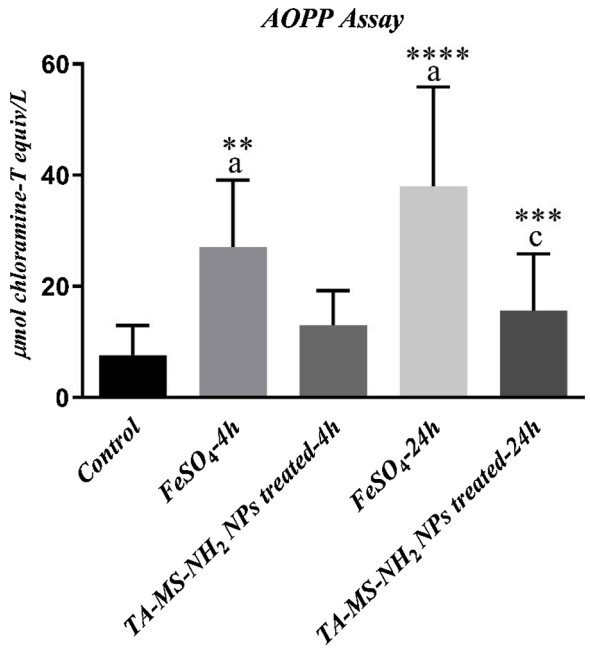

Fig. 7. Effect of TA-MS-NH_2 NPs in iron overload induced hepatotoxicity evaluated by using AOPP level after 4 and 24 h. AOPP level increased in $FeSO_4$-4 h and $FeSO_4$-24 h groups compared with the control group. Treatment with TA-MS-NH_2 NPs after 24 h, meaningfully decreased AOPP levels in TA-MS-NH2 NPs treated-24 h group compared with $FeSO_4$-24 h. Quantitative data are reported as the mean ± standard deviation (SD). a) Significant difference vs. control group, c) Significant difference vs. the $FeSO_4$-24 h group; **, $p < 0.01$ ***, $p < 0.001$ and ****, $p < 0.0001$.

Abbreviations: AOPP: Advanced oxidation protein products; $FeSO_4$: Ferrous sulfate; TA-MS-NH_2 NPs: Amino-functionalized tannic acid-templated mesoporous silica nanoparticles.

protocol introduced by Brand-Williams et al. [30]. Briefly, 250 µL DPPH in ethanol solution was mixed with 5 µL serum samples and 5 µL standard solutions in microplate wells. The solution was shaken well and placed in a dark environment at room temperature. The absorbance rate was recorded after 15 min at a wavelength of 517 nm using a microplate reader (Epoch). Moreover, DPPH values were calculated from standard curves using Trolox as a standard, the results of which were presented as µmol Trolox equiv/L.

2.6.2. Malondialdehyde (MDA) measurement

As a lipid peroxidation marker (LPO), the MDA serum levels were measured via Zantox kits (Birjand, Iran) using the thiobarbituric acid reactive substances (TBARS) method [31]. In short, 100 µL of the samples and standard solutions was added to the tubes. Then, 1000 µL of TBARs reagent and 10 µL of Butylated hydroxytoluene (BHT) solution were also added. The solution was incubated at 96 °C for 20 min and placed in an ice bath for another 10 min. After that, 1100 µL of n-butanol was added and centrifuged at 2000 rpm. Also, the supernatant was used directly to determine MDA, and finally, the absorbance rate was measured at 532 nm. Furthermore, 1,1,3,3 Tetramethoxypropane was used as standard, and the results were presented in µmol/L.

2.6.3. Thiol groups measurement

To measure the concentration of thiol groups, the researchers used Zantox kits (Birjand, Iran) and the Ellman's reagent (5.5′-dithiobis-(2-nitrobenzoic acid) or DTNB) [32]. Briefly, 200 µL of reaction buffer was added to 10 µL of the samples and standard solutions. The absorbance rate was recorded at a wavelength of 412 nm (sample blank absorbance) and, then, 10 µL of DTNB reagent was added to the solution (sample absorbance). Moreover, reduced glutathione was used as a standard. Also, to determine the total thiol concentration (µmol/L), sample blank absorbance was subtracted from the sample absorbance, and, then, the thiol group concentration rate was calculated based on the standard curve. The results were presented in µmol/L.

2.6.4. Measurement of the Advanced Oxidation Protein Products (AOPPs)

AOPP concentration was measured by spectrophotometric methods [33]. The required samples were prepared as follows: Diluted sample (40 µL) was added to each well of a 96-well plate, and the standards of chloramine T (190 µL; 1.25, 2.5, 5, 10, 20, and 40 µM) were added to the plate. Then, 10 µL potassium iodide-KI (1.16 M) and 160 µL citric acid were added to all wells. Moreover, the absorbance of the reaction mixture was measured at a wavelength of 340 nm (OD_{340}) using a spectrophotometer (Epoch). AOPP levels were reported in µmol/L as chloramine-T equivalents.

2.6.5. Total nitrite and nitrate (NOx) measurement

Serum NOx concentrations were measured by ZellBio GmbH (Germany) and the Griess reaction [34]. In brief, 300 µL serum samples and 10 µL sulfanilic acid were centrifuged for 10 min at 3000−4000 rpm. Then, the supernatants were used to determine NOx. Next, 100 µL of supernatant and 100 µL of standards were added to micro wells and which was followed by the addition of 100 µL Griess Reagent [50 µL sulfanilamide (2%) and 50 µL N-(1-Naphthyl) ethylenediamine dihydrochloride (0.1 %)]. Moreover, the absorbance rate was measured after 30 min at a wavelength of 540 nm using the microplate reader (Epoch). Serum NOx level was determined based on the established linear standard curve using sodium nitrate as a standard whose result was presented in µmol/L.

2.7. Statistical analysis

The collected data were analyzed both the SPSS 16.0 software (SPSS

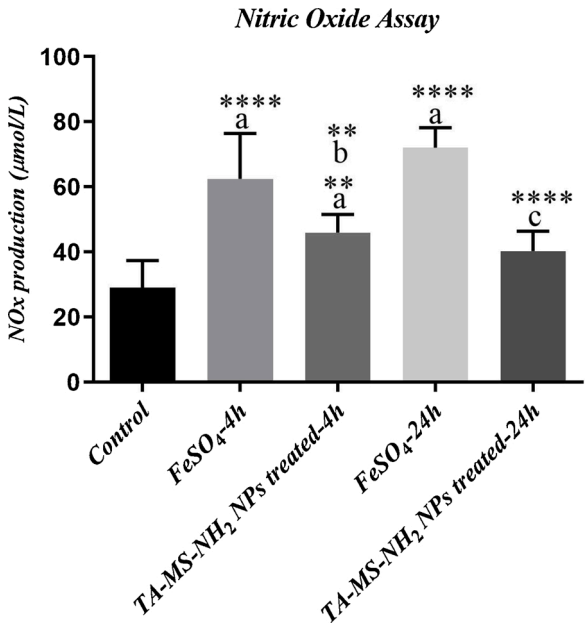

Fig. 8. Effect of TA-MS-NH_2 NPs in iron overload induced hepatotoxicity evaluated by using NOx level after 4 and 24 h. NOx level increased in $FeSO_4$-4 h and $FeSO_4$-24 h groups compared with the control group. Treatment with TA-MS-NH_2 NPs meaningfully decreased the NOx levels in TA-MS-NH2 NPs treated-4 h and TA-MS-NH2 NPs treated-24 h groups compared with the $FeSO_4$-4 h and $FeSO_4$-24 h groups. Quantitative data are reported as the mean-± standard deviation (SD). a) Significant difference vs. control group, b) Significant difference vs. the $FeSO_4$-4 h group, c) Significant difference vs. the $FeSO_4$-24 h group; **, $p < 0.01$ and ****, $p < 0.0001$.

Abbreviations: NOx: Nitric oxide; $FeSO_4$: Ferrous sulfate; TA-MS-NH_2 NPs: Amino-functionalized tannic acid-templated mesoporous silica nanoparticles.

Inc., Chicago, IL, USA) and GraphPad Prism version 6 (San Diego, CA). All statistical analyses were examined via one-way analysis of variance (ANOVA) and Tukey's tests. P-values <0.05 were regarded as statistically significant. The data were presented as mean ± standard deviation.

3. Results

3.1. Characterization of TA-MS-NH_2 NPs

The TA-MS-NH_2 NPs morphological features, size, and shape were examined using FE-SEM and TEM images (Fig. 1A, B). The FE-SEM image showed monodispersed TA-MS-NH_2 NPs with a spherical shape, and TEM images indicated the formation of spherical porous nanoparticles, suggesting that TA-MS-NH_2 NPs are of 140−180 nm size with rough surfaces. Moreover, DLS results showed that TA-MS-NH_2 NPs had an average size of 189.46 ± 1.46 nm and a PDI of 0.039 (Fig. 1C). Additionally, the zeta potential of TA-MS-NH_2 NPs was +23.46 ± 1.72 mV. Also, FT-IR measurement was carried out to show the typical peaks of silica in TA-MS-NH_2 NPs (Fig. 2). Then, the FT-IR peaks at 3430 cm^{-1} were assigned to the stretching vibration of Si—OH and adsorbed water, and the peaks at 1638 cm^{-1} were assigned to bending vibration of water. It was also found that the peaks at 803 cm^{-1} and 468 cm^{-1} corresponded to the symmetric stretching and bending vibration of Si—O—Si, the peaks at 1122 cm^{-1} corresponded to asymmetric stretching of Si-O-Si, and the peaks at 950 cm^{-1} corresponded to symmetric stretching of Si−OH groups [35].

3.2. Effects of TA-MS-NH_2 NPs on serum enzyme levels

Administrating iron in rats significantly increased serum hepatocellular injury biomarker levels (AST, ALT, and ALP). As shown in Fig. 3, while AST and ALT increased at time, the rise of the ALP level was delayed. Moreover, the activity of ALP level in the FeSO4−24 h group was significantly increased compared to the $FeSO_4$-4 h group. On the other hand, although oral administration of TA-MS-NH_2 NPs decreased the levels of serum marker of liver enzymes, it was not significant for the ALP after 4 h.

3.3. Effects of TA-MS-NH_2 NPs on TAC levels

TAC results achieved by applying FRAP and DPPH methods on analyzed samples are reported in Fig. 4A and B. Accordingly, oral administration of $FeSO_4$ led to a time-dependent reduction in FRAP level compared to the control group. On the other hand, 24 h after the administration of TA-MS-NH_2 NPs, the FRAP level was statistically increased (605.7 ± 41.79 µM Fe(II)/L) compared to what obtained for the $FeSO_4$-24 h group (392.1 ± 71.56 µM Fe(II)/L). Moreover, there was no significant difference between TA-MS-NH2 NPs treated-24 h and the control group, indicating these nanoparticles' ability to reduce Fe^{+3} to Fe^{+2}. It was also found that DPPH level was significantly decreased in $FeSO_4$ groups after 4 and 24 h (93.45 ± 57.38 and 58.94 ± 29.56 µmol Trolox equiv/ L, respectively) compared to what experienced by the control group (298.4 ± 78.68 µmol Trolox equiv/L).

As shown in Fig. 4, TA-MS-NH_2 NPs showed significant DPPH radical scavenging properties. Accordingly, DPPH level was statistically increased in 4 h-treated and 24 h-treated TA-MS-NH2 groups (260 ± 69.01, and 241.4 ± 7913 µmol Trolox equiv/L, respectively) in comparison with $FeSO_4$-4 h and $FeSO_4$-24 h groups, respectively. Furthermore, no significant difference was found between the DPPH levels of 4 h-treated and 24 h-treated TA-MS-NH2 NPs and the control group, suggesting these nanoparticles' ability to neutralize free radicals.

3.4. Effects of TA-MS-NH_2 NPs on MDA level

The level of MDA, which is the final product of LPO in the liver tissues, is presented in Fig. 5. The findings of this study also confirmed a significant increase in MDA levels found via TBARS in $FeSO_4$-4 h and $FeSO_4$-24 h groups (0.9775 ± 0.0378 and 1.630 ± 0.3156 µmol/L, respectively) in comparison with the control group (0.6266 ± 0.0689 µM). Following exposure of nanoparticles for 4 h, no significant reduction of MDA levels was observed compared with the control group. However, after 24 h, MDA levels were significantly decreased in TA-MS-NH_2 NPs treated-24 h group (0.9198 ± 0.2431 µM) compared with the $FeSO_4$-24 h group (Fig. 5).

3.5. Effect of TA-MS-NH_2 NPs on thiol level

The level of thiol groups (-SH) was significantly decreased in $FeSO_4$-4 h and $FeSO_4$-24 h groups (273.8 ± 189.7 and 85.81 ± 52.18 µmol/L, respectively) compared with the control group ($p < 0.05$) (484.8 ± 211.6 µmol/L). In contrast, 24 h after the administration of TA-MS-NH_2 NPs, the level of thiol groups was significantly increased in the TA-MS-NH2 NPs treated-24 h group (436.2 ± 48.48 and 495 ± 174 µmol/L) compared with the $FeSO_4$-24 h group. Also, after 24 h, no significant difference was observed in thiol levels between TA-MS-NH2 NPs treated-24 h group and the control groups, indicating the ability of these nanoparticles to increase the level of serum thiol to normal level after 24 h (Fig. 6).

3.6. Effects of TA-MS-NH_2 NPs on AOPP level

As shown in Fig. 7, after oral administration of $FeSO_4$ for 4 and 24 h, the level of serum AOPP was significantly higher in $FeSO_4$-4 h and $FeSO_4$-24 h rats (27.10 ± 12.02 and 38.00 ± 17.85 µmol chloramine T equiv/L, respectively) compared with what observed in the control group (7.628 ± 5.348 µmol chloramine T equiv/L). While there were no

significant differences in serum AOPP levels in the TA-MS-NH2 NPs treated-4 h group, the serum AOPP levels were significantly decreased (15.66 ± 10.21 μmol chloramine T equiv/L) in the TA-MS-NH2 NPs treated-24 h group. Moreover, no significant difference was found in AOPP levels between the TA-MS-NH2 NPs treated-24 h group and the control group.

3.7. Effects of TA-MS-NH_2 NPs on NOx levels

Fig. 8 shows the serum NOx levels in different groups. Compared with the control group (29.04 ± 8.314 μmol/L), the serum NOx levels were found to be higher in $FeSO_4$-4 h and $FeSO_4$-24 h groups (62.47 ± 14.01 and 72.02 ± 6.133 μmol/L, respectively). The results also showed that TA-MS-NH_2 NPs significantly decreased the NOx levels in TA-MS-NH2 NPs treated-4 h and TA-MS-NH2 NPs treated-24 h groups compared with what occurred in $FeSO_4$-4 h and $FeSO_4$-24 h groups (45.97 ± 5.549 and 40.31 ± 6.086 μmol/L, respectively). There was no significant difference in NOx levels between the TA-MS-NH2 NPs treated-24 h group and the control group, indicating the particles' ability to reduce the level of serum NOx in normal level after 24 h.

4. Discussion

As found by many studies, oxidative stress is associated with the pathophysiology of many diseases. According to the findings of different studies, as iron regulate the formation of damaging oxygen radicals and oxidative injury [36,37], its level has a profound effect on various diseases. Moreover, enjoying a supreme capacity to capture heavy metals, TA-MS NPs are appropriate candidates for reducing oxidative stress [38]. Therefore, this study sought to synthesize and characterize the MS NPs using tannic acid as a natural non-surfactant molecule. To this end, as mentioned before, the size of TA-MS-NH_2 NPs was determined through FE-SEM, TEM, and DLS methods.

The FE-SEM and TEM images showed that TA-MS-NH_2 NPs were monodisperse spherical-like particles. The distribution of TA-MS-NH_2 NPs' size, which was measured by DLS, revealed a hydrodynamic diameter. Also, the TA-MS-NH_2 NPs' average size was found to be 189.466 nm with a narrow size distribution. To appraise TA-MS-NH_2 NPs as the potential antioxidant agent, we evaluated the protective role of TA-MS-NH_2 NPs against the oxidative stress changes in iron-induced hepatotoxicity in the serum samples collected from the rat's blood.

According to the study's findings, TA-MS-NH2 NPs reduced iron overload-induced oxidative stress, which is referred to as an imbalance between free radicals and antioxidants and can be measured via oxidative stress-related parameters [39].

The liver is the main human body's storage organ for iron and the excess iron contents involved in liver diseases [40,41]. This study found that the serum levels of AST and ALT were significantly higher in $FeSO_4$-4 h and $FeSO_4$-24 h groups than in the control group and that the ALP level was increased with delay time, which is probably due to the fact that ALP level usually increases late in bile duct damage, which is consistent with the findings of prior studies [42]. Although an increase in levels of hepatocellular enzyme markers has been associated with liver damage [43–45], treatment with TA-MS-NH_2 NPs lowered the hepatic marker enzyme levels to the normal level, proving the hepatoprotective effects of TA-MS-NH_2 NPs on Iron- induced toxicity.

In several studies, TAC has been introduced as one of the leading indicators of oxidative stress [46,47]. Therefore, this study measured TAC through DPPH and FRAP assays. TAC_{FRAP} is a measurement used for the compounds with reducing power, and TAC_{DPPH} is a measurement used for the compounds with radical scavenging capacity [48]. Based on the FRAP results of the serums collected from rats which had received TA-MS-NH_2 NPs, a robust antioxidant activity was found in those groups compared to the $FeSO_4$ group. Furthermore, the DPPH assay confirmed a significant antioxidant activity of TA-MS-NH_2 NPs, indicating its direct role in removing the exposed radicals. Therefore, the TA-MS-NH_2 NPs exhibited free radical scavenging activities and reduced the ferric ion to ferrous ion. It should be noted that intense LPO caused by an iron overload may affect the cytoplasmic membranes and mitochondrial, damage the tissues, and release lipid hydroperoxides into blood circulation, reflecting the induction of oxidative stress [49,50].

Iron overload is known as a stimulator of LPO in hepatocytes that increases the risk of hepatic injury [51]. Thus, in this study, the level of MDA was also measured as the end product of lipid peroxidation. The findings of this research are consistent with the previous studies in terms of the effect of iron overload-induced LPO compared with healthy control groups [52]. On the other hand, the significantly lower MDA levels in serums of TA-MS-NH2 NPs treated-24 h group compared with the FeSO4−24 h group suggest lipid peroxidation attenuation. The thiol redox status in plasma, especially thiol (–SH) groups of protein, is considered important antioxidants under in vivo conditions [53]. Thiol-containing biomolecules are required to be protected against the unfavorable effects of oxidative stress [54]. According to the previous studies, iron has a strong affinity to the sulfhydryl (–SH) groups of several antioxidant enzymes, and thus, it can alter antioxidant activities by inhibiting their functional SH groups. Consistent with the findings of Guzelcicek [55], the present study showed that increased levels of iron were associated with reduced thiol levels. It was also found that the administration of TA-MS-NH_2 NPs increased the thiol level compared to $FeSO_4$-4 h and $FeSO_4$-24 h groups in a time-dependent manner.

Recent studies have confirmed the significance of AOPP as a marker of oxidative stress and the end product of free radicals on proteins [56]. According to the results, the serum AOPP levels significantly increased in $FeSO_4$-4 h and $FeSO_4$-24 h groups than in the control group. These findings are in agreement with Drüeke et al. [57] and Kisic et al. [58] studies that found an increase in the level of AOPP in plasma of the patients with end-stage renal disease, showing a direct association between serum ferritin and AOPP concentrations, and between intravenous administration of Iron and AOPP levels. Nevertheless, 24 h after administrating TA-MS-NH_2 NPs, the AOPP level in the rats' serum which received $FeSO_4$ was statistically reduced.

Another important parameter in examining oxidative stress is the NOx level which was evaluated in the serums of all groups [59]. The oral administration of FeSO4 increased the serum NOx levels in a time-dependent manner. A similar study by Videla et al. [60] reported that the iron overload led to the generation of ROS and that it was associated with nitric oxide metabolites' levels and oxidative stress. Following the treatment with TA-MS-NH_2 NPs after 24 h, a significant reduction in NOx level was observed in comparison with $FeSO_4$ groups, showing these particles' ability to reduce the level of serum NOx at a normal level.

5. Conclusion

According to the study's results, it can be concluded that the protective effect of TA-MS-NH_2 NPs against hepatic injury in iron-treated rats is possibly related to their antioxidant features. TA-MS-NH_2 NPs could be an effective and promising treatment for iron overload. This study clearly showed that TA-MS-NH_2 NPs had hepatoprotective application in preventing or minimizing iron-induced liver damage.

Conflict of Interest

The authors declare no conflict of interest.

Declaration of Competing Interest

The authors report no declarations of interest.

Acknowledgments

The authors of this study would like to express their profound

gratitude to Birjand University of Medical Sciences, Birjand, Iran, for financially supporting this study.

References

[1] S. Dev, J.L. Babitt, Overview of iron metabolism in health and disease, Hemodial. Int. 21 (2017) S6–S20.
[2] R.N. Musacco Sebio, C.M. Saporito Magriñá, J.M. Acosta, A.A. Boveris, M. G. Repetto, Iron and Copper Toxicity in Rat Liver: a Kinetic and Holistic Overview, 2017.
[3] A. Pietrangelo, Mechanisms of iron hepatotoxicity, J. Hepatol. 65 (2016) 226–227.
[4] J.R. Waymack, M. Tweet, R. Austin, Iron overdose, J. Educ. Teach. Emergency Med. 4 (2019).
[5] D. Ansong, C. Nkyi, C.O. Appiah, E.X. Amuzu, C.A. Frimpong, I. Nyanor, S. B. Nguah, J. Sylverken, Epidemiology of paediatric poisoning reporting to a tertiary hospital in Ghana, S. Afr. J. Child Health 10 (2016) 68–70.
[6] S. Puntarulo, Iron, oxidative stress and human health, Mol. Aspects Med. 26 (2005) 299–312.
[7] S.J. Dixon, B.R. Stockwell, The role of iron and reactive oxygen species in cell death, Nat. Chem. Biol. 10 (2014) 9.
[8] V. Berdoukas, T.D. Coates, Z.I. Cabantchik, Iron and oxidative stress in cardiomyopathy in thalassemia, Free Radic. Biol. Med. 88 (2015) 3–9.
[9] M. Schieber, N.S. Chandel, ROS function in redox signaling and oxidative stress, Curr. Biol. 24 (2014) R453–R462.
[10] X. Chai, D. Li, X. Cao, Y. Zhang, J. Mu, W. Lu, X. Xiao, C. Li, J. Meng, J. Chen, ROS-mediated iron overload injures the hematopoiesis of bone marrow by damaging hematopoietic stem/progenitor cells in mice, Sci. Rep. 5 (2015) 10181.
[11] D.F. Wallace, The regulation of iron absorption and homeostasis, Clin. Biochem. Rev. 37 (2016) 51.
[12] N. Mobarra, M. Shanaki, H. Ehteram, H. Nasiri, M. Sahmani, M. Saeidi, M. Goudarzi, H. Pourkarim, M. Azad, A review on iron chelators in treatment of iron overload syndromes, Int. J. Hematol. Stem Cell Res. 10 (2016) 239.
[13] J.C. Barton, Optimal management strategies for chronic iron overload, Drugs 67 (2007) 685–700.
[14] R. Narayan, U.Y. Nayak, A.M. Raichur, S. Garg, Mesoporous silica nanoparticles: a comprehensive review on synthesis and recent advances, Pharmaceutics 10 (2018) 118.
[15] M.Y. Hanafi-Bojd, L. Ansari, B. Malaekeh-Nikouei, Codelivery of anticancer drugs and siRNA by mesoporous silica nanoparticles, Ther. Deliv. 7 (2016) 649–655.
[16] N. Hao, H. Yang, L. Li, L. Li, F. Tang, The shape effect of mesoporous silica nanoparticles on intracellular reactive oxygen species in A375 cells, New J. Chem. 38 (2014) 4258–4266.
[17] J.-k. Gao, Z.-j. Zhang, Y.-j. Jiang, Y. Chen, S.-f. Gao, Biomimetic-functionalized, tannic acid-templated mesoporous silica as a new support for immobilization of NHase, Molecules 22 (2017) 1597.
[18] J.-B. Pang, K.-Y. Qiu, Y. Wei, A new nonsurfactant pathway to mesoporous silica materials based on tartaric acid in conjunction with metallic chloride, Chem. Mater. 13 (2001) 2361–2365.
[19] L. Bau, B. Bartova, M. Arduini, F. Mancin, Surfactant-free synthesis of mesoporous and hollow silica nanoparticles with an inorganic template, Chem. Commun. (2009) 7584–7586.
[20] Z. Gao, I. Zharov, Large pore mesoporous silica nanoparticles by templating with a nonsurfactant molecule, tannic acid, Chem. Mater. 26 (2014) 2030–2037.
[21] R.G. Andrade Jr., L.T. Dalvi, J.M.C. Silva Jr., G.K. Lopes, A. Alonso, M. Hermes-Lima, The antioxidant effect of tannic acid on the in vitro copper-mediated formation of free radicals, Arch. Biochem. Biophys. 437 (2005) 1–9.
[22] G.K. Lopes, H.M. Schulman, M. Hermes-Lima, Polyphenol tannic acid inhibits hydroxyl radical formation from Fenton reaction by complexing ferrous ions, Biochim Biophys Acta Gen. Subj. 1472 (1999) 142–152.
[23] R.G. Andrade Jr., J.S. Ginani, G.K. Lopes, F. Dutra, A. Alonso, M. Hermes-Lima, Tannic acid inhibits in vitro iron-dependent free radical formation, Biochimie 88 (2006) 1287–1296.
[24] T. Basu, S. Panja, A.K. Shendge, A. Das, N. Mandal, A natural antioxidant, tannic acid mitigates iron-overload induced hepatotoxicity in Swiss albino mice through ROS regulation, Environ. Toxicol. 33 (2018) 603–618.
[25] N. Sahiner, S. Sagbas, N. Aktas, Preparation and characterization of monodisperse, mesoporous natural poly (tannic acid)–silica nanoparticle composites with antioxidant properties, Microporous Mesoporous Mater. 226 (2016) 316–324.
[26] Y. Jiang, W. Sun, L. Zhou, L. Ma, Y. He, J. Gao, Improved performance of lipase immobilized on tannic acid-templated mesoporous silica nanoparticles, Appl. Biochem. Biotechnol. 179 (2016) 1155–1169.
[27] H. Javdani, R. Khosravi, L. Etemad, M. Moshiri, A. Zarban, M.Y. Hanafi-Bojd, Tannic acid-templated mesoporous silica nanoparticles as an effective treatment in acute ferrous sulfate poisoning, Microporous Mesoporous Mater. 307 (2020), 110486.
[28] I.F. Benzie, J.J. Strain, The ferric reducing ability of plasma (FRAP) as a measure of "antioxidant power": the FRAP assay, Anal. Biochem. 239 (1996) 70–76.
[29] A. Gupta, R. Kumar, R. Ganguly, A.K. Singh, H.K. Rana, A.K. Pandey, Antioxidant, anti-inflammatory and hepatoprotective activities of Terminalia bellirica and its bioactive component ellagic acid against diclofenac induced oxidative stress and hepatotoxicity, Toxicol. Rep. 8 (2021) 44–52.
[30] W. Brand-Williams, M.-E. Cuvelier, C. Berset, Use of a free radical method to evaluate antioxidant activity, LWT-Food Sci. Technol. 28 (1995) 25–30.
[31] K. Yagi, A simple fluorometric assay for lipoperoxide in blood plasma, Biochem. Med. (Zagreb) 15 (1976) 212–216.
[32] S.I. Ojeaburu, K. Oriakhi, Hepatoprotective, antioxidant and, anti-inflammatory potentials of gallic acid in carbon tetrachloride-induced hepatic damage in Wistar rats, Toxicol. Rep. 8 (2021) 177–185.
[33] V. Witko, A.T. Nguyen, B. Descamps-Latscha, Microtiter plate assay for phagocyte-derived Taurine-chloramines, J. Clin. Lab. Anal. 6 (1992) 47–53.
[34] K.M. Miranda, M.G. Espey, D.A. Wink, A rapid, simple spectrophotometric method for simultaneous detection of nitrate and nitrite, Nitric Oxide 5 (2001) 62–71.
[35] M.Y. Hanafi-Bojd, M.R. Jaafari, N. Ramezanian, M. Xue, M. Amin, N. Shahtahmassebi, B. Malaekeh-Nikouei, Surface functionalized mesoporous silica nanoparticles as an effective carrier for epirubicin delivery to cancer cells, Eur. J. Pharm. Biopharm. 89 (2015) 248–258.
[36] J.G. Fischer, H.P. Glauert, T. Yin, M.L. Sweeney-Reeves, N. Larmonier, M.C. Black, Moderate iron overload enhances lipid peroxidation in livers of rats, but does not affect NF-κB activation induced by the peroxisome proliferator, Wy-14,643, J. Nutr. 132 (2002) 2525–2531.
[37] N. Bresgen, P.M. Eckl, Oxidative stress and the homeodynamics of iron metabolism, Biomolecules 5 (2015) 808–847.
[38] J. Gao, H. Lei, Z. Han, Q. Shi, Y. Chen, Y. Jiang, Dopamine functionalized tannic-acid-templated mesoporous silica nanoparticles as a new sorbent for the efficient removal of Cu 2+ from aqueous solution, Sci. Rep. 7 (2017) 45215.
[39] M.A. Sánchez-Rodríguez, V.M. Mendoza-Núñez, Oxidative stress indexes for diagnosis of health or disease in humans, Oxid. Med. Cell. Longev. 2019 (2019).
[40] A. Pietrangelo, Iron and the liver, Liver Int. 36 (Suppl. 1) (2016) 116–123.
[41] S. Pelusi, L. Valenti, S. Fargion, Oxidative stress and hepatic iron overload. Studies on Hepatic Disorders, Springer, 2015, pp. 345–356.
[42] A. Glance, Special considerations in interpreting liver function Te, Am. Fam. Physician 59 (1999) 2223–2230.
[43] L. Pari, A. Karthikeyan, P. Karthika, A. Rathinam, Protective effects of hesperidin on oxidative stress, dyslipidaemia and histological changes in iron-induced hepatic and renal toxicity in rats, Toxicol. Rep. 2 (2015) 46–55.
[44] R. Sarkar, B. Hazra, N. Mandal, Hepatoprotective potential of Caesalpinia crista against iron-overload-induced liver toxicity in mice, Evid. Complement. Alternat. Med. 2012 (2012).
[45] G.I. Al-Basher, Green tea activity and iron overload induced molecular fibrogenesis of rat liver, Saudi J. Biol. Sci. (2017).
[46] A.M. Pisoschi, G.P. Negulescu, Methods for total antioxidant activity determination: a review, Biochem. Anal. Biochem. 1 (2011) 106.
[47] J.O. Costa, C.M.P. Vásquez, G.d.J. Santana, N.d.J. Silva, J.d.M. Braz, A.M. Jesus, D. G.d. Silva, L.C.S. Cunha, K.B.F. Barbosa, Plasma total antioxidant capacity and cardiometabolic risk in non-obese and clinically healthy young adults, Arq. Bras. Cardiol. 109 (2017) 140–147.
[48] D. Ştef, I. Gergen, T. Traşcă, Ş.L. Monica Hărmănescu, B. Ramona, M. Hegheduş, Total antioxidant and radical scavenging capacities for different medicinal herbs, Rom. Biotechnol. Lett. 14 (2009) 4705–4710.
[49] B.R. Bacon, R. O'Neill, C.H. Park, Iron-induced peroxidative injury to isolated rat hepatic mitochondria, Free Radic. Biol. Med. 2 (1986) 339–347.
[50] J. Yang, G. Zhang, D. Dong, P. Shang, Effects of Iron overload and oxidative damage on the musculoskeletal system in the space environment: data from spaceflights and ground-based simulation models, Int. J. Mol. Sci. 19 (2018) 2608.
[51] B.R. Bacon, R.S. Britton, Hepatic injury in chronic iron overload. Role of lipid peroxidation, Chem.-Biol. Interact. 70 (1989) 183–226.
[52] B. Ćurko-Cofek, T.G. Kezele, J. Marinić, M. Tota, N.S. Čizmarević, Č. Milin, S. Ristić, B. Radošević-Stašić, V. Barac-Latas, Chronic iron overload induces gender-dependent changes in iron homeostasis, lipid peroxidation and clinical course of experimental autoimmune encephalomyelitis, Neurotoxicology 57 (2016) 1–12.
[53] P. Mungli, M.S. Shetty, P. Tilak, N. Anwar, Total thiols: biomedical importance and their alteration in various disorders, Online J. Health Allied Sci. 8 (2009).
[54] S. Toyokuni, Iron and thiols as two major players in carcinogenesis: friends or foes? Front. Pharmacol. 5 (2014) 200.
[55] A. Guzelcicek, G. Cakirca, O. Erel, A. Solmaz, Assessment of thiol/disulfide balance as an oxidative stress marker in children with β-thalassemia major, Pak. J. Med. Sci. 35 (2019) 161.
[56] G. Güntaş, B. Engin, Ö.B. Ekmekçi, Z. Kutlubay, H. Ekmekci, A. Songür, T.K. Ü. Uzunçakmak, H.E. Vehid, S. Serdaroğlu, Y. Tüzün, Evaluation of advanced oxidation protein products, prooxidant-antioxidant balance, and total antioxidant capacity in untreated vitiligo patients, Ann. Dermatol. 27 (2015) 178–183.
[57] T. Drucke, V. Witko-Sarsat, Z. Massy, Iron therapy, AOPP, and carotid artery IMT in end-stage renal disease, Circulation 106 (2002) 2212–2217.
[58] B. Kisic, D. Miric, R. Stolic, A. Ilic, J. Rasic, M. Miric, I. Dragojevic, Investigation of lipid peroxidation products and antioxidant enzyme activities in end-stage renal disease patients, Adv. Chem. Eng. Sci. 2014 (2013).
[59] D. Pierini, N.S. Bryan, Nitric oxide availability as a marker of oxidative stress. Advanced Protocols in Oxidative Stress III, Springer, 2015, pp. 63–71.
[60] L.A. Videla, V. Fernández, G. Tapia, P. Varela, Oxidative stress-mediated hepatotoxicity of iron and copper: role of Kupffer cells, Biometals 16 (2003) 103–111.